

# Wigner crystallization in the two electron quantum dot

A. Matulis

*Institute of Semiconductor Physics, Goštauto 11, 2600 Vilnius, Lithuania*

F. M. Peeters<sup>†</sup>

*Departement Natuurkunde, Universiteit Antwerpen (UIA), Universiteitsplein 1, B-2610 Antwerp, Belgium*

(November 21, 2018)

Wigner crystallization can be induced in a quantum dot by increasing the effective electron-electron interaction through a decrease of the electron density or by the application of a strong magnetic field. We show that the ground state in both cases is very similar but the energy scales are very different and therefore also the dynamics.

PACS numbers: 73.20.Dx, 85.30.Vw, 03.65.-w

## I. INTRODUCTION

During the last ten years quantum dots have attracted a lot of interest both experimentally and theoretically [1]. Recently, much attention was paid to the investigation of quantum dots in strong perpendicular magnetic fields where a rich structure of cusps and steps in the chemical potential  $\mu(N, B)$  (as a function of confined electron number  $N$  and applied magnetic field strength  $B$ ) was observed [2]. The above structure is related to changes in the ground state electron density in the presence of a magnetic field, and it initiated numerous theoretical investigations after Chamon and Wen [3] proposed the quantum dot edge reconstruction. The electron density in a quantum dot is the result of the interplay of the repulsive character of the electron interaction and the attractive forces caused by the confining potential, the magnetic field and the electron exchange interaction. If the magnetic field is strong enough, the overlap between the electron wave functions becomes less, the electron interaction will dominate, and a ring of electrons at the dot edge is formed. It was also found that if the magnetic field is increased further the above electron ring becomes unstable, and a ground state with a broken rotational symmetry appears. The possibility of the appearance of spin waves [4] and charge density waves [5,6] have also been reported.

A quantum dot with a density profile consisting of rings with lumps reminds us to the Wigner crystal [7,8] which is the ground state of the classical electron system in a dot [9] in the absence of a magnetic field. In the latter case the Wigner crystal occurs when the potential energy (the inter-electron interaction and the confinement potential) dominates over the electron kinetic energy. This is just the classical limit in a quantum problem. Therefore, classical or quasi-classical methods should be adequate for

the description of the Wigner crystal. But from a first sight it appears that such a classical limit is not reached when a strong magnetic field is applied. The above mentioned electron density reconstruction was revealed when the magnetic field is so strong that the electrons occupy the lowest Landau level. Thus, the electron motion quantization is essential, and consequently, the kinetic energy exceeds the potential energy due to the Coulomb interaction. Nevertheless, due to the degeneracy of the Landau level this large electron kinetic energy is actually frozen out, and Wigner crystallization results from the same potential energy as in the classical case without magnetic field. Actually the above crystallization is a result of different energy scales in the electron system under consideration.

The purpose of the present paper is, by using an exactly solvable model of two electrons in a dot, to illustrate the conditions under which a Wigner crystal can be formed in the case of a strong magnetic field ( $B$ ), and to compare this quantum Wigner crystal with the classical zero magnetic field one. The paper is organized as follows. In Sect. II we present our model. Sect. III gives an introduction to the quasi-classical approach for the  $B = 0$  case. Sect. IV discusses the general  $B \neq 0$  case. Our conclusions are presented in Sect. V.

## II. MODEL

We consider two electrons with effective masses  $m^*$  moving in the  $z = 0$  plane and which are confined by a two-dimensional harmonic potential of characteristic frequency  $\omega_0$ . A magnetic field is applied in the  $z$  direction and described by the vector potential chosen in the symmetric gauge  $\mathbf{A} = [\mathbf{B} \times \mathbf{r}]/2$ . The corresponding Hamiltonian can be separated into two parts

$$H = H_R + H_r, \quad (1)$$

(see, for instance [10,11]) which represents the center-of-mass and relative motion (with corresponding coordinates  $\mathbf{R} = (\mathbf{r}_1 + \mathbf{r}_2)/2$  and  $\mathbf{r} = \mathbf{r}_1 - \mathbf{r}_2$ ). In dimensionless form those parts can be written as follows:

$$H_R = -\frac{1}{4}\nabla_R^2 + \left\{1 + \frac{B^2}{4}\right\}R^2 - \frac{iB}{2}[\mathbf{R} \times \nabla_R]_z, \quad (2a)$$

$$H_r = -\nabla_r^2 + \frac{1}{4}\left\{1 + \frac{B^2}{4}\right\}r^2 - \frac{iB}{2}[\mathbf{r} \times \nabla_r]_z + \frac{\lambda}{r}. \quad (2b)$$

The system energy is measured in  $\hbar\omega_0$  units, and the coordinates in  $a_0 = \sqrt{\hbar/m^*\omega_0}$  units. The symbol  $\lambda = a_0/a_B$  stands for the electron interaction coupling constant which is the ratio of the characteristic dot dimension  $a_0$  and the Bohr radius  $a_B = \epsilon\hbar^2/m^*e^2$ . The magnetic field strength  $B$  is measured in  $\Phi_0/\pi a_0^2$  units where  $\Phi_0 = \pi\hbar c/e$  is the magnetic flux quantum.

We will concentrate ourselves to the study of the coordinate wave function part of the ground singlet state

$$\Psi(\mathbf{r}_1, \mathbf{r}_2) = \Phi(\mathbf{R})\psi(\mathbf{r}), \quad (3)$$

the corresponding electron density

$$\begin{aligned} \rho(\mathbf{r}) &= \int d^2r_1 \int d^2r_2 |\Psi(\mathbf{r}_1, \mathbf{r}_2)|^2 \hat{\rho}(\mathbf{r}) \\ &= \int d^2r_1 \int d^2r_2 |\Psi(\mathbf{r}_1, \mathbf{r}_2)|^2 \sum_{n=1}^2 \delta(\mathbf{r} - \mathbf{r}_n) \\ &= 2 \int d^2r_1 |\Phi(\mathbf{r} + \mathbf{r}_1/2)|^2 |\psi(\mathbf{r}_1)|^2 \end{aligned} \quad (4)$$

and the correlation function

$$\begin{aligned} K(\mathbf{r}, \mathbf{r}') &= \int d^2r_1 \int d^2r_2 |\Psi(\mathbf{r}_1, \mathbf{r}_2)|^2 \\ &\quad \times \{\hat{\rho}(\mathbf{r})\hat{\rho}(\mathbf{r}') - \delta(\mathbf{r} - \mathbf{r}')\hat{\rho}(\mathbf{r})\} \\ &= 2|\Phi(\{\mathbf{r} + \mathbf{r}'\}/2)|^2 |\psi(\mathbf{r} - \mathbf{r}')|^2. \end{aligned} \quad (5)$$

It is the latter function which enables one to determine whether, or not the system is in the Wigner crystal state.

### III. ZERO MAGNETIC FIELD CASE

We consider first the simplest case in which no magnetic field is applied. Then the center-of-mass motion part is trivial. It just represents the two dimensional harmonic oscillator motion which has no relation to the Wigner crystallization problem. Its ground state energy is  $E_R = 1$  with the corresponding wave function

$$\Phi(\mathbf{R}) = \sqrt{\frac{2}{\pi}} \exp(-R^2). \quad (6)$$

Due to the cylinder symmetry the relative motion wave function part can be written as

$$\psi(\mathbf{r}) = \frac{1}{\sqrt{2\pi}} \exp(im\varphi)R(r), \quad (7)$$

where the radial function  $R(r)$  is obtained by solving the one dimensional eigenvalue problem as determined by the Hamiltonian

$$H_r = -\frac{1}{r} \frac{d}{dr} r \frac{d}{dr} + V(r, \lambda), \quad (8a)$$

$$V(r, \lambda) = \frac{m^2}{r^2} + \frac{1}{4}r^2 + \frac{\lambda}{r}. \quad (8b)$$

As was already mentioned strong electron correlation (and the Wigner crystal as well) occurs when the potential energy dominates over the electron kinetic energy, i. e. when  $\lambda \rightarrow \infty$ . In this interesting limit the eigenvalue problem is strongly simplified and can be solved by analytical means. Indeed, in the case of  $\lambda \rightarrow \infty$  the potential (8b) has a minimum close to the point  $r_0 = (2\lambda)^{1/3}$  (see solid curve in Fig. 1). The potential can be expanded into a  $(r - r_0)$  series (dashed curve in Fig. 1)

$$V(r, \lambda) \approx \frac{3}{4}(2\lambda)^{2/3} + \frac{3}{4}(r - r_0)^2 + \frac{m^2}{(2\lambda)^{2/3}}, \quad (9)$$

which actually coincides with the quasi-classical expansion into a  $\lambda^{-2/3}$  series [11]. The form of the above expansion clearly indicates the energy scales of the different excitations in the quantum dot. The first term ( $\lambda^{2/3}$ ) is just the classical dot energy which can also be obtained using the hydrodynamic approximation [12]. In the  $\lambda \rightarrow \infty$  limit this energy dominates. Thus, we are in the region of the classical Wigner crystal. The solution of the Schrödinger equation with the harmonic term in the expansion of the potential (9) leads to  $\lambda$ -independent equidistant electron ring vibration excitations (shown in Fig. 1 by the horizontal dashed lines). Note that the separation of those vibration levels are of order 1, and consequently, much less than the classical potential energy. The last term in the expansion (9) describes the rotation energy. It leads to a small (of order  $\sim \lambda^{-2/3}$ ) splitting of the rotation levels as is shown by the encircled part in Fig. 1 which is enlarged. The spectrum is thus similar to the one of molecules with bands of rotation levels, attached to each vibration level.

For the expanded potential (9) we obtain the following quasi-classical radial ground state wave function,

$$P(r) = N \exp\{-a(r - r_0)^2\}, \quad (10)$$

where  $a = \sqrt{3}/4$  and the normalization  $N = (2a/\pi)^{1/4} r_0^{-1/2}$ .

Inserting the above relative motion wave function (10) together with the center-of-mass motion function (6) into expressions (4,5) we obtain the electron density

$$\begin{aligned} \rho(r, \varphi) &= \frac{2N^2}{\pi^2} \int_0^\infty dr' r' \exp(-2r^2 - r'^2/2) \\ &\quad \times \exp\{-2a(r' - r_0)^2\} \int_0^{2\pi} d\varphi' \exp\{2rr' \cos(\varphi - \varphi')\} \\ &= \frac{4N^2}{\pi} \int_0^\infty dr' r' \exp\{-2r^2 - r'^2/2 - 2a(r' - r_0)^2\} \\ &\quad \times I_0(2rr') \approx \frac{N^2}{\pi} \sqrt{\frac{2\gamma}{a}} \exp\{-\gamma(r - r_0/2)^2\}, \end{aligned} \quad (11)$$

and the correlation function

$$\begin{aligned} K(\mathbf{r}, \mathbf{r}') &= \frac{4N^2}{\pi} \exp\{-(\mathbf{r} + \mathbf{r}')^2/2\} \\ &\quad \times \exp\{-2a(|\mathbf{r} - \mathbf{r}'| - r_0)^2\}. \end{aligned} \quad (12)$$

In expression (11),  $I_0$  is the Bessel function and  $\gamma = 8a/(1+4a) \approx 1.268$ .

A schematic picture of the above functions is shown in Fig. 2 by the shadowed regions. In Fig. 2(a) the electron density is depicted which is mainly concentrated on a thin ring. Notice that it has no lumps, and exhibits the cylindrical symmetry of the system Hamiltonian. Wigner crystal state can be seen in the correlation function [13,14] which is plotted in Fig. 2(b). The latter is actually the same as the conditional probability distribution. One electron is fixed in position  $\mathbf{r}'$  (indicated by a cross in Fig. 2(b)) and the density of the other electron is then mainly concentrated in the opposite position which clearly indicates the presence of Wigner crystallization in this quasi-classical limit.

#### IV. STRONG MAGNETIC FIELD CASE

Due to the symmetric gauge which preserves the cylindrical symmetry, both (i. e. center-of-mass and relative) wave functions can be written as a product of the orbital exponent and the radial part as in expression (7). The corresponding radial Hamiltonians (for center-of-mass and relative motions) can be presented as follows:

$$H_R = -\frac{1}{4} \frac{d}{dR} R \frac{d}{dR} + \frac{1}{4} \left( \frac{M}{R} - BR \right)^2 + R^2, \quad (13a)$$

$$H_r = -\frac{1}{r} \frac{d}{dr} r \frac{d}{dr} + \left( \frac{m}{r} - \frac{Br}{4} \right)^2 + \frac{1}{4} r^2 + \frac{\lambda}{r}. \quad (13b)$$

Because we are interested in the asymptotic limit  $B \rightarrow \infty$ , it is convenient to scale the variables and the Hamiltonian as follows

$$\mathbf{r} \rightarrow \mathbf{r} B^{-1/2}, \quad \mathbf{R} \rightarrow \mathbf{R} B^{-1/2}, \quad H \rightarrow HB, \quad (14)$$

in order to have the expansion parameter  $B^{-1}$  explicitly in our problem. Inserting (14) into expression (13) we arrive at the following Hamiltonian:

$$H_R = -\frac{1}{4} \frac{d}{dR} R \frac{d}{dR} + \frac{1}{4} \left( \frac{M}{R} - R \right)^2 + V_R(R, B), \quad (15a)$$

$$H_r = -\frac{1}{r} \frac{d}{dr} r \frac{d}{dr} + \left( \frac{m}{r} - \frac{r}{4} \right)^2 + V_r(r, B), \quad (15b)$$

where in the asymptotic region  $B \rightarrow \infty$  the terms

$$V_R(R, B) = \frac{R^2}{B^2}, \quad (16a)$$

$$V_r(r, B) = \frac{r^2}{4B^2} + \frac{\lambda}{r\sqrt{B}} \quad (16b)$$

can be treated as small perturbations.

The solution of the Schrödinger equations for the zero order Hamiltonians (without the terms  $V_R$  and  $V_r$ ) leads to the degenerate Landau levels where the ground state

has energy  $E_R = E_r = 1/2$  labeled by integer positive momentum ( $M$  and  $m$ ) values. Mathematically this degeneracy is a consequence of the equivalence of the zero center-of-mass Hamiltonian potential  $(M/R - R)^2/4$  which is shown in Fig. 3(a) where the orbital momentum is indicated by the corresponding integers. For any momentum  $M$  the potential curve has a minimum equal to zero at the position  $R_{\min} = \sqrt{M}$ . A similar potential is obtained for the zero order relative motion equation, and will therefore not be discussed.

Next we take the perturbation terms into account. For the case of center-of-mass motion the potential is shown in Fig. 3(b). The potential is composed of the same curves as in the case without perturbation, but they are now moved up by the amount  $R^2/B^2$  shown in Fig. 3(b) by the dotted curve. The lowest minimum is obtained for  $M = 0$  which implies that the center-of-mass motion wave function is the same as in the case without magnetic field (6).

This is not the case for the relative motion where all potential curves are shifted up by the amount  $V_r(r, B)$  as shown in Fig. 3(c) by the dotted curve. According to Eq. (16b) this curve increases for both  $r \rightarrow 0$  and  $r \rightarrow \infty$  and reaches a minimum value at

$$r_{\min} = (2\lambda)^{1/3} \sqrt{B}. \quad (17)$$

Minimizing the potentials with respect to the relative angular momentum for  $r = r_{\min}$  we obtain the corresponding orbital momentum

$$m = \left( \frac{\lambda}{4} \right)^{2/3} B. \quad (18)$$

Consequently, the relative motion wave function is peaked on the ring of radius  $r_0$ . When the magnetic field strength increases the radius  $r_0$  tends to infinity, while the orbital number is growing as well. Expanding the potential with the lowest minimum in the vicinity of the equilibrium point (17) we find

$$\left( \frac{m}{r} - \frac{r}{4} \right)^2 \approx \frac{(r - r_{\min})^2}{4}, \quad (19)$$

which means that the thickness of the ring remains constant.

The layout of the energy spectrum in the large magnetic field limit is shown in Fig. 4. Notice that the spectrum has two different energy scales as in the  $B = 0$  case. But the physical meaning of those scales is quite different. The largest energy scale is the electron kinetic energy. And the rotation levels are split due to the interplay of the Coulomb interaction between the electrons and the confinement potential.

Going back to our original units before the scaling (14) we find that the ring radius is  $r_{\min} = (2\lambda)^{1/3}$ , which is identical to the zero magnetic field case. But now the thickness of the ring is  $\sim B^{-1/2}$ , and it tends to zero as the magnetic field strength approaches infinity.

Surprisingly, we arrived at the same situation as was found for the case without magnetic field. The relative motion wave function is located on a ring whose diameter greatly exceeds its thickness. Thus the conclusions of previous section concerning Wigner crystallization in the quantum dot are also valid in the strong magnetic field case. While for  $B = 0$  the Wigner crystal state is reached for  $\lambda \gg 1$  we find that a sufficiently strong magnetic field can crystallize the system for any  $\lambda \neq 0$ .

## V. CONCLUSIONS

The occurrence of Wigner crystallization depends on the ratio of the distance between the electrons ( $l$ ) and the characteristic dimension of the single electron wave packet ( $a$ ). Actually this ratio is a measure of the electron density in the quantum dot. In our case  $l$  is given by the radius  $r_{\min}$  of the ring in the correlation function, and  $a$  coincides with its thickness. This ratio is

$$\chi = \frac{l}{a} = \frac{r_{\min}}{a} = \frac{\lambda^{1/3}}{B^{-1/2}} = \lambda^{1/3} \sqrt{B}, \quad (20)$$

which in real units reads

$$\chi = \left( \frac{a_0}{a_B} \right)^{1/3} \left( \frac{a_0}{l_B} \right). \quad (21)$$

Here  $l_B = \sqrt{\hbar c / eB}$  is the magnetic length.

The larger this ratio the more pronounced the Wigner crystal state is. Thus, both a strong magnetic field and strong interaction favors Wigner crystallization, but in a different way. The electron interaction makes the system less dense by enlarging the inter-particle distance. The magnetic field also makes the system effectively less dense but by compressing the single electron wave packages.

Also we would like to note that mathematically in both cases the static Wigner crystal properties can be calculated by the same method, namely by the minimization of the classical potential energy which is composed of the electron interaction and the confinement potential. Nevertheless the physical meaning of that calculation is quite different. In the strong electron interaction case the potential energy dominates making the whole problem quasi-classical, while in the case of strong magnetic fields, the problem is essentially quantum mechanical (the Landau level energy is dominating). But due to the degeneracy of the problem the system is guided by the same potential energy as for the  $B = 0$  case but with different energy scales. Therefore, although the Wigner crystal configuration is the same, one can expect different dynamics in the two limiting cases.

## ACKNOWLEDGMENTS

This work is supported by the Flemish Science Foundation, IUAP-VI and the "Bijzonder Onderzoeksfonds van

de Universiteit Antwerpen". One of us (F. M. P.) is a research director with FWO-VI. We acknowledge discussions with B. Partoens, S. Reimann and D. Pfannkuche.

---

<sup>†</sup> Electronic address: peeters@uia.ua.ac.be

- [1] L. Jacak, P. Hawrylak, and A. Wójs, *Quantum Dots* (Springer-Verlag, Berlin Heidelberg, 1998).
- [2] T. H. Oosterkamp, J. W. Janssen, L. P. Kouwenhoven, D. G. Austing, T. Honda, and S. Tarucha, *Phys. Rev. Lett.* **82**, 2931 (1999).
- [3] C. de C. Chamon and X. G. Wen, *Phys. Rev.* **49**, 8227 (1994).
- [4] M. Koskinen, M. Manninen, and S. M. Reimann, *Phys. Rev. Lett.* **79**, 1389 (1997).
- [5] K. Hirose, and Ned S. Wingreen, *Phys. Rev. B* **59**, 4604 (1999).
- [6] S. M. Reimann, M. Koskinen, and M. Manninen, *Phys. Rev. Lett.* **83**, 3270 (1999).
- [7] H.-M. Müller and E. Koonin, *Phys. Rev. B* **54**, 14532 (1996).
- [8] E. Goldmann and S. R. Renn, *Phys. Rev. B* **60**, 16611 (1999).
- [9] V. M. Bedanov and F. M. Peeters, *Phys. Rev. B* **49**, 2667 (1994).
- [10] U. Merkt, J. Huser, and M. Wagner, *Phys. Rev. B* **43**, 7320 (1991).
- [11] A. Matulis and F. M. Peeters, *J. Phys.:Condens. Matter* **6**, 7751 (1994).
- [12] Z. L. Ye and E. Zaremba, *Phys. Rev. B* **50**, 17217 (1994).
- [13] P. A. Maksym, *Physica B* **184**, 385 (1993).
- [14] C. Yannouleas and U. Landman, cond-mat/0002364.
- [15] P. A. Maksym, *Phys. Rev. B* **53**, 10871 (1996).

FIG. 1. The potential energy for the relative motion (solid curve) and its quadratic expansion (dashed curve) around its minimum (9). The horizontal lines are the different vibration levels in units of  $\hbar\omega_0$ .

FIG. 2. Schematic view of the electron density (a) and the electron correlation function (b) in the quasi-classical limit.

FIG. 3. The potential energy curves for different angular momentum in case of: (a) the non-interacting problem, (b) the center-of-mass motion including confinement, and (c) the relative motion including confinement and electron-electron interaction.

FIG. 4. Energy spectrum in the limit of a strong magnetic field. The energy is given in units of  $\hbar\omega_c$ .

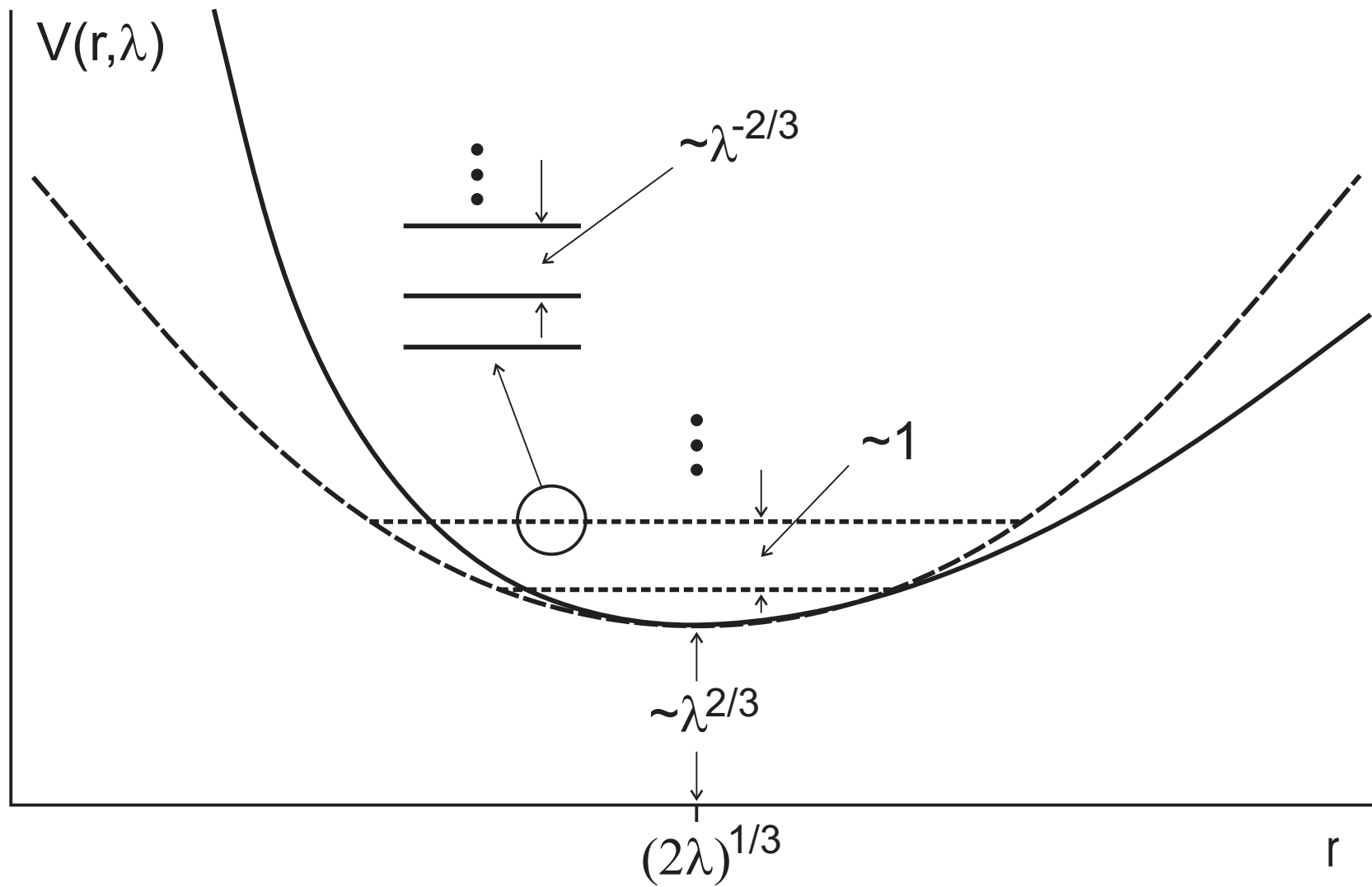
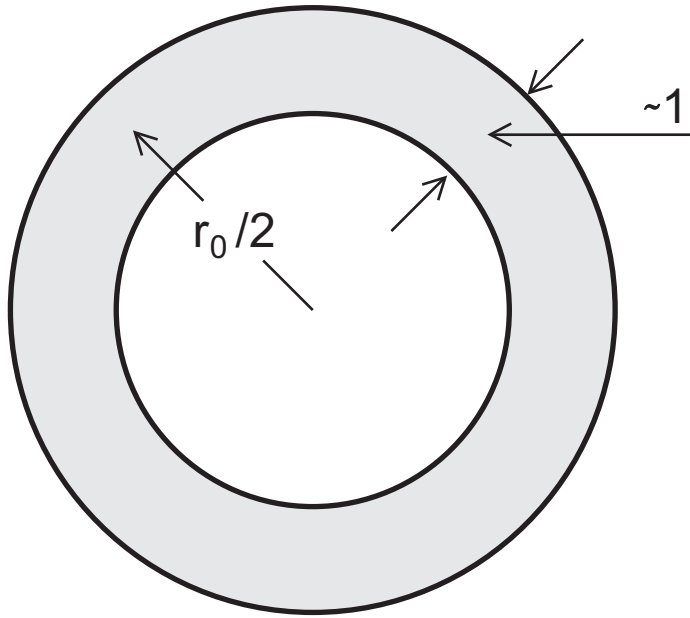
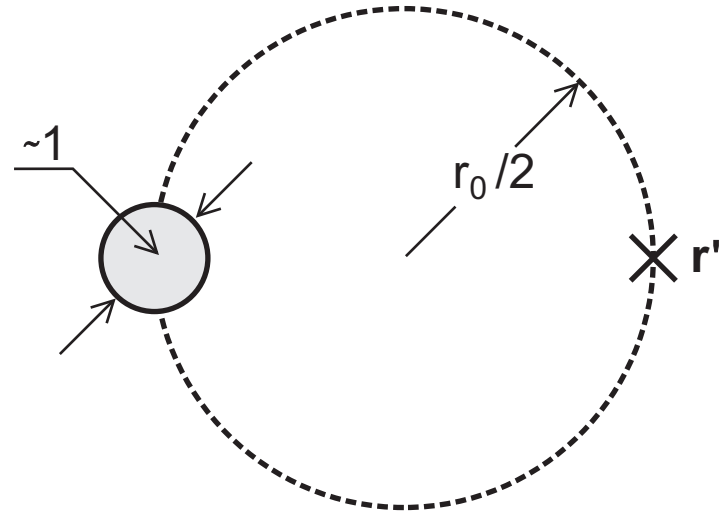


Fig. 1



(a)



(b)

Fig. 2

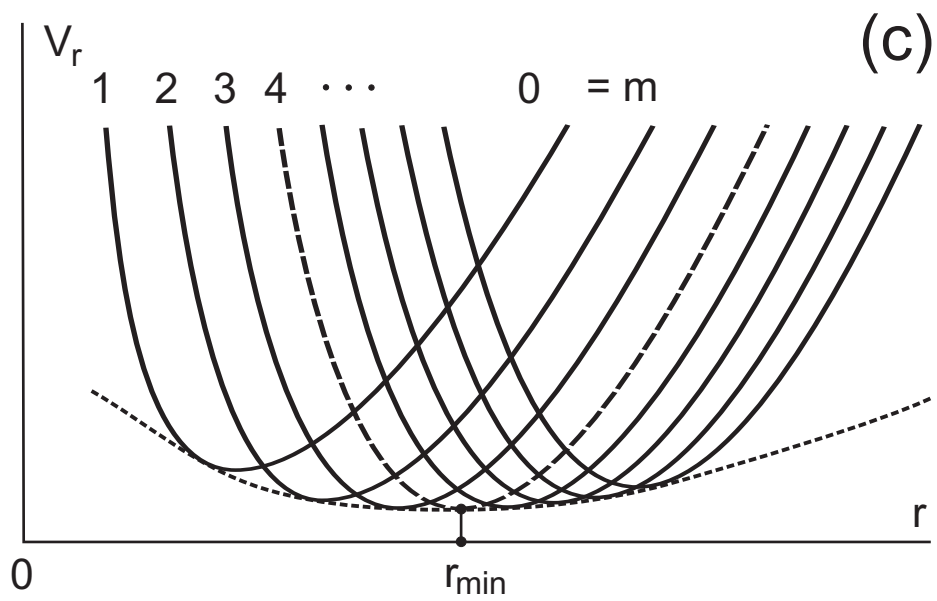
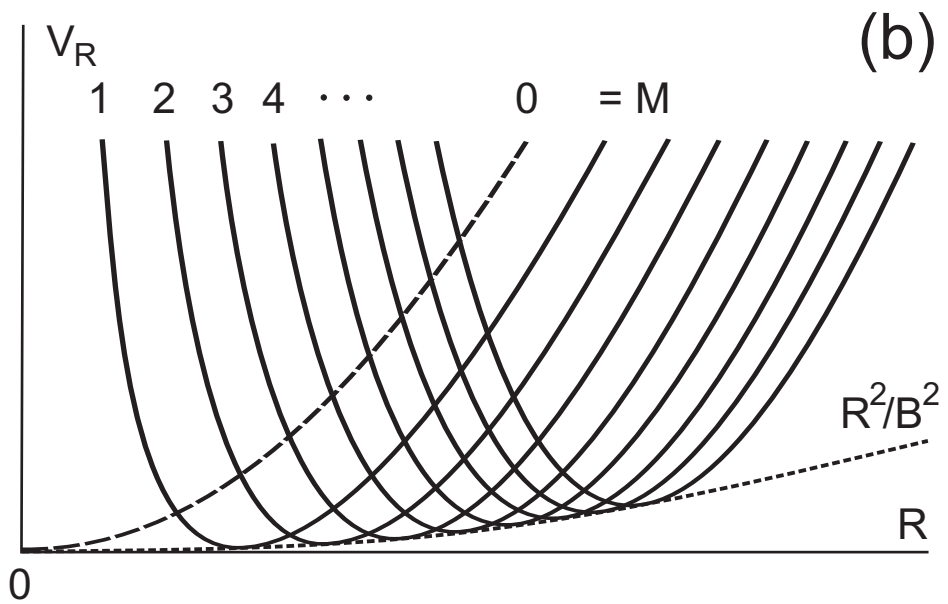
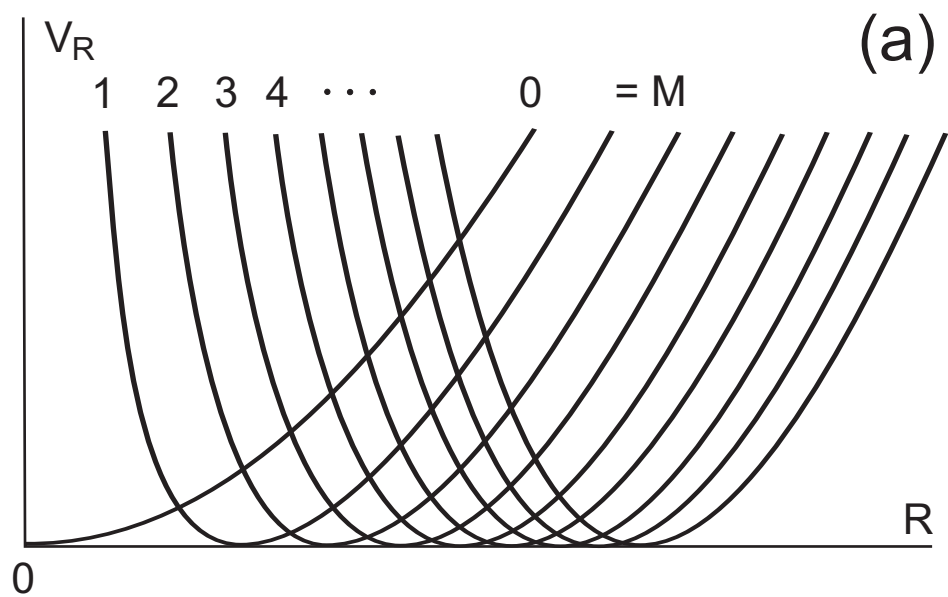


Fig. 3



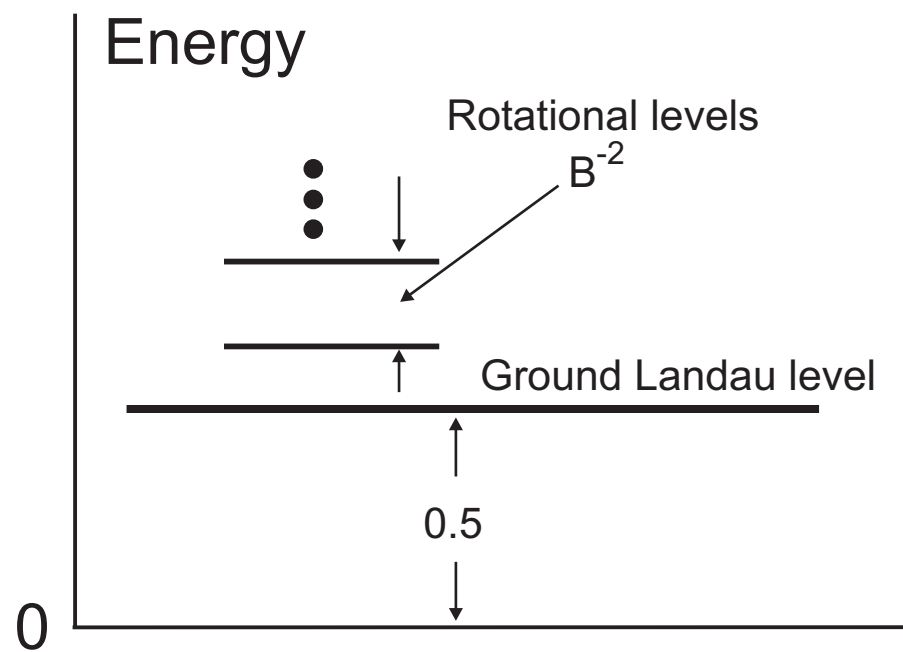


Fig. 4